Electrodiffusion and electroconvection in *Sn* In and *Sn* Sb dilute liquid alloys

D. Agnoux, J. M. Augeard, J. M. Escanyé, and M. Gerl
Laboratoire de Physique des Solides, Université Nancy I, Case Officielle 140, 54037 Nancy-Cedex, France*
(Received 30 January 1978)

The effective diffusion coefficient D_{eff} and the apparent effective valence Z^{**} of In and Sb as dilute impurities in liquid Sn have been measured using a shear cell device. D_{eff} is shown to vary quadratically as a function of the current density j (A cm^{-2}): $D_{\text{eff}}^{\text{In}} = 4.4\times10^{-5} + 1.22\times10^{-8} j^2$ ($\text{cm}^2\text{sec}^{-1}$). A possible origin of the electroconvective enhancement of the diffusion coefficient is discussed. The effective valences $Z_{\text{In}}^{**} = +1.4\pm0.9$; $Z_{\text{Sb}}^{**} = -4.2\pm4$ are in good agreement with theoretical calculations.

I. INTRODUCTION

Although electrodiffusion in liquid metals has been the subject of considerable study,[1] the results appear rather scattered and a detailed theoretical description of the mechanisms of electroconvection is still lacking. The process of electromigration leading to a relative drift of the solute with respect to the solvent is comparatively better understood, and a number of papers have been devoted to its theoretical description in solids and liquids.[2-9] As shown in these papers, the net driving force on each ion in a binary mixture is made up of two contributions: (i) the direct electrostatic force exerted by the mean electric field $\vec{E}$ on the bare ion of charge Z_α, and (ii) the friction force due to electron-ion interactions, a part of which is cancelling the electrostatic force. The net driving force on each atom of species α is usually written

$$\vec{F}_\alpha = Z_\alpha^* |e| \vec{E}, \tag{1}$$

and Z_α^* is called the effective valence of species α in the mixture.

As both the friction force and the impurity resistivity arise from a momentum transfer from the conduction electron gas to the ion, there is a close connection between Z_α^* and the specific resistivity ρ_α of species α in the solvent. For instance, it has been shown from general considerations[6] that in dilute alloys

$$Z_\alpha^* = -n_0(\rho_\alpha/\rho), \tag{2}$$

where $\rho = \rho_0 + n_\alpha \rho_\alpha$ is the total resistivity of the alloy containing n_α impurities and n_0 conduction electrons per unit volume.

In most experiments, however, diffusion in liquid alloys takes place in a closed capillary, and, because of the coupling between the diffusion of the two components, an apparent effective valence Z_α^{**} is measured. We show in Sec. IV of the present paper that

$$Z_\alpha^{**} = Z_\alpha^* - (V_\alpha/V_s) Z_s^*, \tag{3}$$

where Z_α^* and Z_s^* are the effective valences of solute and solvent, respectively, and V_α and V_s their partial atomic volumes in the binary mixture.

It is in principle straightforward to deduce Z_α^{**} from a measurement of the apparent drift velocity $\vec{v}_\alpha$ of the solute in the laboratory frame, as $\vec{v}_\alpha$ is related to the apparent driving force $Z^{**}|e|\vec{E}$ by the Nernst-Einstein equation

$$\vec{v}_\alpha = (D_\alpha/kT) Z_\alpha^{**} |e| \vec{E}, \tag{4}$$

where D_α is the diffusion coefficient of species α.

In addition to this effect that leads to impurity segregation, it has been shown experimentally[10-16] that, even in thin capillaries, an electric current induces hydrodynamic convection in the system. Because of this electroconvective effect, the apparent diffusion coefficient D_{eff} is the sum of D, the usual diffusion coefficient due to random atomic displacements and $D_c(j)$, a convective contribution to D_{eff}. Attempts have been made to describe quantitatively this effect, but no completely satisfactory explanation has yet been given.

In Sec. II of the present paper, we describe the apparatus used to measure D_{eff} and Z_α^{**} in the dilute alloys *Sn*In and *Sn*Sb. We show that D_{eff} varies quadratically as a function of j the current density in the sample, and we give an explanation of this behavior based on surface effects. Section IV is devoted to measurements of Z^{**} for Sb and In impurities in liquid tin and to a general comparison between experimental data published on a number of alloys and the theoretical formula (3).

II. EXPERIMENTAL PROCEDURE

In most experiments published in the literature,[17,18] a capillary-reservoir technique is used to determine the diffusion and electrodiffusion coefficients. This method presents major draw-

backs as: (i) atomic diffusion occurs when heating the sample up to the temperature of the experiment and when cooling it back to room temperature so that large corrections must be made to account for these effects, and (ii) solute segregation may occur when solidification of the sample takes place. In our method, described elsewhere,[19,20] the use of a shear-cell device avoids these drawbacks. The cell is made of a stacking of 15 boron-nitride disks, 4 mm thick, in which four capillaries, 1.5 mm in diameter, are bored. The mechanical arrangement of the system allows rotating the disks with respect to each other from outside the furnace (the geometry is reminiscent of that of a variable capacitor). A typical experiment proceeds as follows: (i) the capillaries are initially filled with liquid tin of 99.999% purity and a dilute alloy of tin with a radioactive isotope of the solute is inserted in an intermediate disk, without contact with the solvent; (ii) when the desired temperature and current density are obtained in the capillaries, this intermediate disk is rotated and contact between the thin layer of radioactive alloy with the two halves of each capillary determines the beginning of the diffusion run; and (iii) at the end of the run each disk is rotated with respect to its neighbors; hence, each capillary is sectioned into 15 beads which are subsequently extracted from the disks, and whose radioactivity is measured using a standard NaI-(Tl) γ analyzer.

The solute concentration $c_\alpha(x,t)$ along each sample is the solution of the Fick equation

$$\frac{\partial c_\alpha}{\partial t} = D_{\text{eff}} \frac{\partial^2 c_\alpha}{\partial x^2} - v_\alpha \frac{\partial c_\alpha}{\partial t} \tag{5}$$

subjected to the boundary conditions:

$$\text{(a)}\quad c_\alpha(x,0) = c_0 \Theta(x+h)[1-\Theta(x-h)]\,, \tag{6}$$

where $2h$ is the thickness of the intermediate disk, Θ is the step function, and c_0 is the initial solute concentration in this disk; (b) at the upper end of the sample, the capillaries end into the filling reservoir, then

$$c_\alpha(\infty,0) = \frac{\partial c_\alpha(\infty,0)}{\partial x} = 0\,;$$

(c) at the bottom of the sample where the capillaries are closed by the lower electrode, a condition of zero flux is used

$$-D_{\text{eff}} \frac{\partial c_\alpha}{\partial x} + v_\alpha c_\alpha = 0\,.$$

The diffusion coefficient D_{eff} and the drift velocity v_α are obtained using a least-squares fitting of the experimental data to the solution of (5) (see Fig. 1).

In the present paper we report measurements of D_{eff} and Z^{**} performed on the dilute alloys $Sn\,Sb^{124}$, $Sn In^{111}$, and $Sn In^{115}$ (a ionic-microprobe analysis being used for determining the concentration of ^{115}In).

III. EFFECTIVE DIFFUSION COEFFICIENT AND ELECTROCONVECTION

A. Experimental data

The experimental data obtained in the present paper (Figs. 2 and 3, Tables I and II) show that there is no threshold for the appearance of electroconvection, in disagreement with the results of Belaschenko[11] but in agreement with Shaw and Verhoeven.[12] For a current density as small as 50 A cm^{-2} in the *Sn*Sb alloy for instance, the apparent diffusion coefficient is more than twice its value in absence of an electric current. It is apparent on Fig. 3 that in *Sn*In alloys, D_{eff} increases proportionally to j^2, the square of the current density, according to the law

$$D_{\text{eff}}\,(\text{cm}^2\,\text{sec}^{-1}) = (4.4 \pm 0.4)\times 10^{-5} + (1.22 \pm 0.02)\times 10^{-8} j^2\,, \tag{7}$$

when j is given in A cm^{-2}. In *Sn*Sb alloys, D_{eff} varies also as j^2 with a coefficient of the same order of magnitude as for *Sn*In alloys. This shows it is likely that the enhancement of D, when an electric current is passed through the sample, is due to a collective motion of the host liquid, induced by the electric current.

Another systematic feature of electroconvection is the occurrence of transient phenomena: for short runs, some irregularities in concentration profiles and a second peak are observed which cannot be explained using Fick's equation (5). These singularities are not observed in long runs and appear only when the current density is larger than a critical value, namely about 200 A cm^{-2} in *Sn*In and 100 A cm^{-2} in *Sn*Sb alloys. To our knowledge, this phenomenon has not been reported in the literature, although it is very reproducible in our experiments. As the peak always occurs in the lower part of the capillaries, it may be due to a coupling between the electric field and the relative density difference between solute and solvent (7.2% in *Sn*Sb, 0.3% in *Sn*In).

B. Interpretation

In order to interpret the (linear) variation of D_{eff} with the square of the current density in the low-j regime, we assume that a hydrodynamic stationary-convective motion takes place in the liquid metal when an electric current is passed through

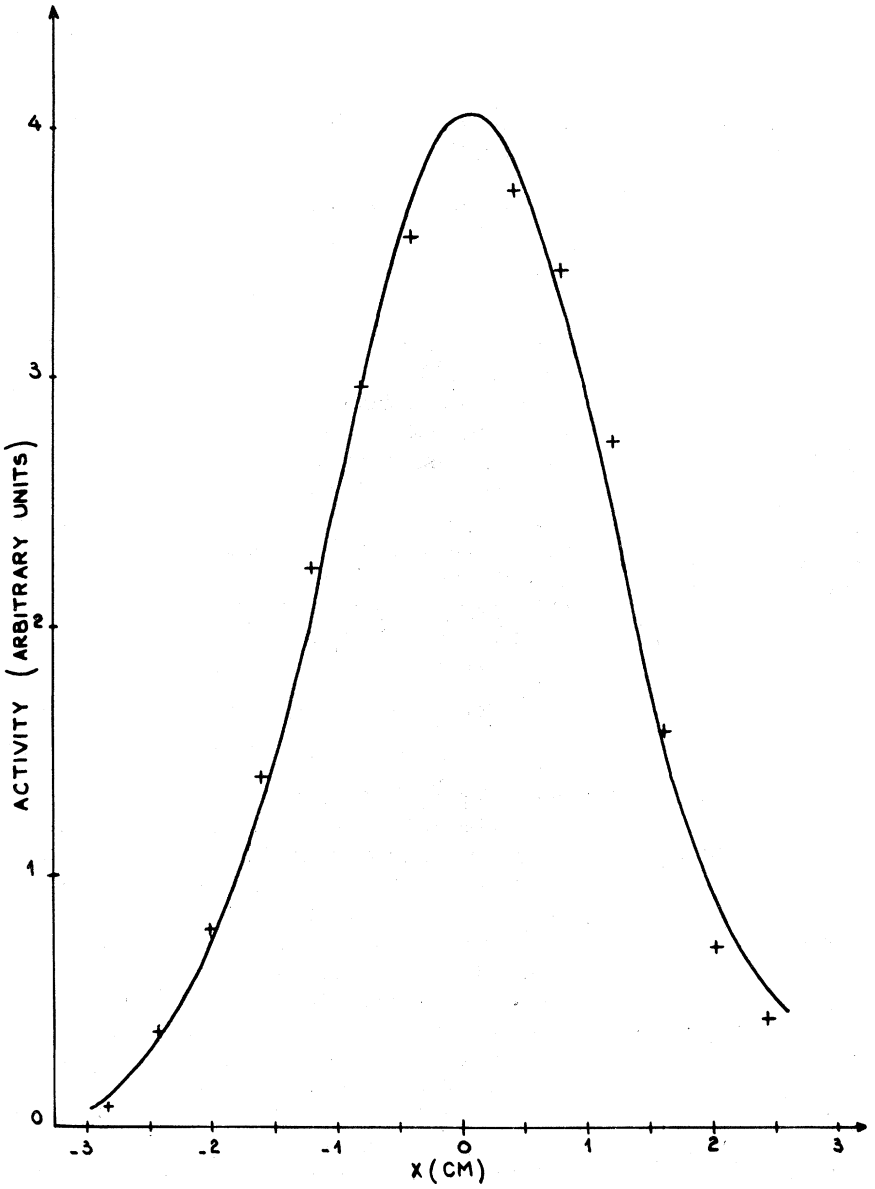

FIG. 1. Typical variation of the activity (arbitrary units) of sections along the capillary; experimental conditions: *Sn* In^{111}, t = 2820 sec, T = 401 °C, j = 120 A cm^{-2}.

the sample. Assuming that the convective velocity $v(r)$ has no azimuthal dependence, it is straightforward to show that the enhancement of the diffusion coefficient[21-23]

$$D_c(j) \sim \frac{2}{D_0 a^2} \int_0^a \frac{dr}{r} \left(\int_0^r v(r') r' \, dr' \right)^2 , \tag{8}$$

where D_0 is the atomic diffusion coefficient and a is the radius of the capillary.

In the literature the origin of this hydrodynamic motion has been traced to (i) inelastic scattering of electrons on the walls of the capillary,[14,16] (ii) magnetohydrodynamics (MHD) effects due to surface irregularities of the capillary[14]; (iii) coupling with the magnetic field[11]; (iv) temperature gradients induced by Joule heating of the sample.[13,15] Among these possible explanations only the first one (i) leads to a quadratic dependence of D_c on j, but D_c is four orders of magnitude too low to account for the experimental law (7). However, influenced by the fact that this interpretation leads to a quadratic variation of $D_c(j)$, we have performed a calculation of the convective velocity based on surface effects. We assume that the number (n_i) of ions per unit volume is constant throughout the sample, up to a the radius of the capillary, and that the number (n_e) of electrons per unit volume varies rapidly in the vicinity of external surfaces according to the law

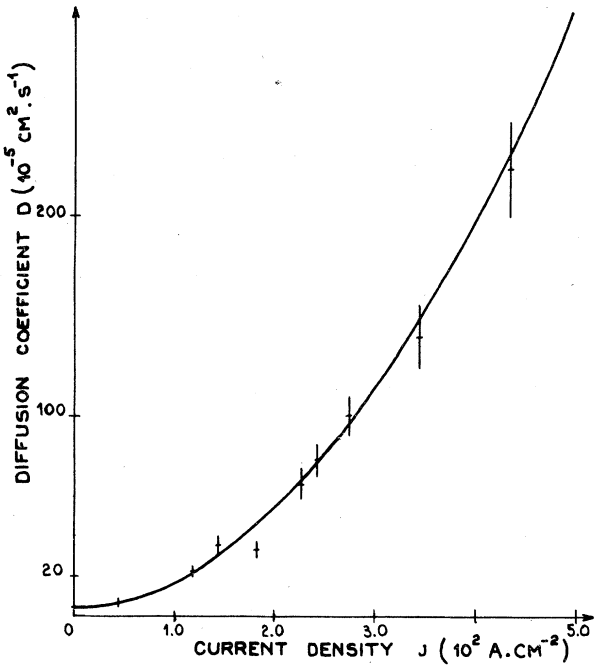

FIG. 2. Plot of the experimental effective diffusion coefficient D (10^{-5} cm^2 sec^{-1}) vs current density j (10^2A cm^{-2}). All measurements are made at an average temperature of 401 °C.

$$n_e(r) = Zn_i\{1 - \tfrac{1}{2}\exp[(r-a)/L]\}\,. \tag{9}$$

This spatial variation of n_e can be traced to: (i) an intrinsic contribution due to the spilling of electrons out of the sample or, (ii) a term due to surface irregularities of the capillary, reducing the electric current near the capillary wall. In Eq. (9), the small distance L is considered as an adjustable parameter in the calculation.

The force on the solvent ions contained in a unit volume of the system can be written

$$f(r) = \{Zn_i - [\alpha n_e(r)/\rho]\}|e|E\,, \tag{10}$$

where Z is the bare charge of a solvent ion and α is the electron drag parameter.[7] As the liquid is in equilibrium on a macroscopic scale, the balance of forces on a section S of the capillary can be written

$$\int_0^a [f(r) - \nabla p]r\,dr = 0\,, \tag{11}$$

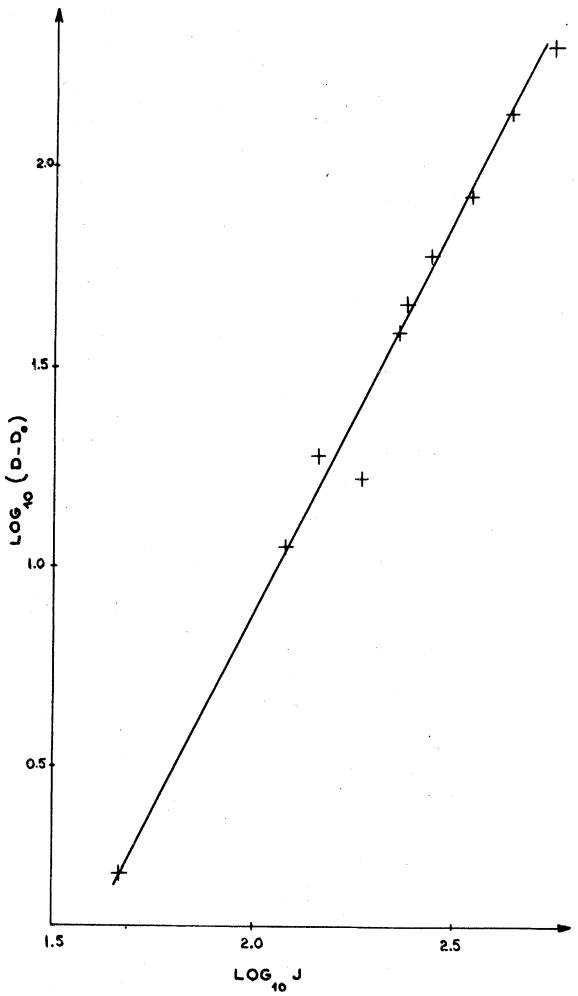

FIG. 3. Log-log plot of the enhancement $(D-D_0)$ of the diffusion coefficient versus current density. The slope of the straight line is equal to 2.0.

where ∇p is the gradient of the electroosmotic pressure along the x axis of the capillary.

We now write the Navier-Stokes equations for the velocity components and we assume: (i) that the velocity $\vec{v}$ of the fluid is parallel to the capillary axis so that p is invariant in a section of the capillary, and (ii) that the capillary is very long so that the velocity of the fluid does not depend on x. From this last condition, $\nabla p = \partial p/\partial x$ is

TABLE I. Experimental data for the electrodiffusion of dilute In in liquid tin.

T (°C)	406	406	403	401	400	400	399	398	400	397	404	407
t (10^3 sec)	6.3	6.3	3.6	2.82	2.1	6.3	1.2	0.6	1.68	0.9	0.9	0.3
j (A cm^{-2})	0	0	46.4	120.0	143.7	186.7	227.5	243.3	275.0	346.3	435.7	547.0
D_{eff} (10^{-5} cm^2 sec^{-1})	4.7	4.0	7.1	22.3	34.8	30.9	65.9	77.6	99.7	139.7	224.4	325.0

independent of x and, to first order in (L/a) Eq. (11) leads to

$$\nabla p = Z|e|En_i(1-\alpha/\rho)\,, \tag{12}$$

and

$$f(r) - \nabla p = A\exp[(r-a)/L]\,, \tag{13}$$

where

$$A = \tfrac{1}{2}Z|e|En_i(\alpha/\rho)\,. \tag{14}$$

The Navier-Stokes equation for the x component of the velocity

$$\Delta v = -(1/\eta)(f-\nabla p)$$

can now be formally solved

$$v(\vec{r}) = \iint_S -(1/\eta)G(\vec{r},\vec{r}')[f(r')-\nabla p]\,d\vec{r}'\,, \tag{15}$$

where $G(\vec{r},\vec{r}')$ is the Green's kernel of the operator Δ appropriate to the boundary conditions relevant to the problem

$$G(\vec{r},\vec{r}') = \begin{cases} \dfrac{1}{2\pi}\ln\left(\dfrac{|\vec{r}-\vec{r}'|}{(r/a)|\vec{r}'-\vec{r}(a^2/r^2)|}\right), & (r\neq 0) \\ \dfrac{1}{2\pi}\ln\left(\dfrac{r'}{a}\right), & (r=0)\,. \end{cases} \tag{16}$$

Using (16) and (13) allows solving (15) for the velocity $v(\vec{r})$ but the nonanalyticity of $G(\vec{r},\vec{r}')$ leads to integration difficulties. Instead of calculating (15) we prefer to assume a plausible velocity profile across the capillary and we choose, as did Pikus and Fiks[16]

$$v(r) = v(0)[1-2r^2/a^2] \quad (0\leq r\leq a-L)\,, \tag{17}$$

$v(r)$ varying rapidly from $-v(0)$ to 0 in the interval $(a-L,a)$. Hence, the velocity profile is entirely determined by $v(0)$ the velocity on the capillary axis

$$v(0) = -\frac{1}{\eta}\int_0^a [f(r')-\nabla p]\ln\frac{r'}{a}r'\,dr'\,. \tag{18}$$

Using the expression (13) for $[f(r')-\nabla p]$, it is straightforward to show that

$$v(0) = (A/\eta)a^2[(L/a)^2 + O(L/a)^3] \tag{19}$$

and, from Eq. (8)

$$D_c(j) = (1/192D_0)(Z|e|n_i\alpha/\eta)^2a^2j^2L^4\,. \tag{20}$$

Using values appropriate to liquid tin, namely, $Z=4$, $D_0 = 4.4\times10^{-5}$ cm^2 sec^{-1}, $n_i = 3.54\times10^{22}$ cm^{-3}, $\alpha = 47.2$ $\mu\Omega$ cm, $\eta = 1.4$cp, $a = 0.75$ mm, our experimental value $D_c(j)/j^2 = 1.22\times10^{-8}$ A^{-2}cm^6 sec^{-1} is obtained when the value $L = 42$ Å is assumed. It is thus apparent that this rather large value cannot be attributed to simple surface effects, but rather to geometrical irregularities on the capillary surface.

TABLE II. Experimental data for the electrodiffusion of dilute Sb in liquid tin.

T (°C)	401	401	404	402
t (10^3 sec)	6.3	3.6	3.54	2.4
j (A cm^{-2})	0	49.7	210.2	313.1
D_{eff} (10^{-5} cm^2 sec^{-1})	3.7	10.1	67.2	47.8

IV. APPARENT EFFECTIVE VALENCE OF In AND Sb OF In AND Sb IN LIQUID TIN

The determination of the apparent effective valence Z_α^{**} of solute ions is made difficult by: (i) the large diffusivity of the solute which limits the duration of the experiments; (ii) the small value of the effective valence of the solute ions; and (iii) the finite thickness of the disks in the shear cell used in the present work. Hence, shifts of the solute distribution smaller than 0.2 cm cannot be easily detected, resulting in an uncertainty of about 60% on the measurements of Z_α^{**}. However, as our experimental method visualizes directly the concentration profile of the solute, we feel confident in our results, in the limits of this uncertainty. The experimental data recorded in Tables III and IV and the following results are obtained:

$$Z_{\text{In}}^{**} = +1.4\pm0.9, \quad Z_{\text{Sb}}^{**} = -4.2\pm4.0\,. \tag{21}$$

In order to make contact with theoretical calculations, we recall that the effective valence Z_i^* and Z_s^* of solute and solvent atoms in a binary mixture can be defined as the flux J_q of electric charge driven by a unit flux of the component i (or s) when no electric field is applied to the

TABLE III. Measurements of the apparent effective valence of ^{111}In (a) and ^{115}In (b) isotopes in liquid tin. The resistivity of the alloy has been always taken as $\rho_{400} = 50$ $\mu\Omega$ cm. The average of the effective valence is $Z_{\text{In}}^{**} = +1.4 \pm 0.9$.

T (°C)	j (A cm^{-2})	t (sec)	X (cm)	Z^{**}
408 (b)	70.2	6300	0.14	+2.33
405 (b)	129.0	6300	0.31	+1.54
400 (a)	143.7	2100	0.20	+2.16
404 (b)	151.7	6300	0.28	+1.30
400 (a)	186.7	6300	0.30	+0.96
405 (b)	199.2	6300	0.81	+1.42
399 (a)	227.5	1200	0.10	+0.59
398 (a)	243.3	600	0.13	+1.34
411 (b)	254.6	6300	1.5	+1.12
400 (a)	275.0	1680	0.83	+2.10
404 (a)	435.7	900	0.72	+0.95

TABLE IV. Measurements of the apparent effective valence of ^{124}Sb, averaging to $Z^{**}_{Sb} = -4.2 \pm 4.00$.

T (°C)	j (A cm^{-2})	t (sec)	X (cm)	Z^{**}
402	94.9	2700	-0.28	-8.5
404	210.2	3300	-1.05	-3.0
402	313.1	2400	-0.89	-1.1

system[6]

$$|e|Z_i^* = \left(\frac{J_q}{J_i}\right)_{J_S=0,\ E=0}\ ;\quad |e|Z_s^* = \left(\frac{J_q}{J_s}\right)_{J_i=0,\ E=0}.$$

When both components are allowed to diffuse in the alloy in absence of any external electric field the total flux of charge is therefore

$$(J_q)_{E=0} = (J_i Z_i^* + J_s Z_s^*)|e| . \tag{22}$$

In our experiments, diffusion takes place in a closed capillary and volume conservation of the alloy implies that

$$J_i V_i + J_s V_s = 0 , \tag{23}$$

where V_i and V_s are the partial atomic volumes of solvent and solute atoms, respectively, whose number per unit volume is N_i and N_s

$$N_i V_i + N_s V_s = 1 . \tag{24}$$

J_i and J_s are therefore not independent, and the net flux of charge driven by a unit flux of the solute

$$|e|Z_i^{**} = \left(\frac{J_q}{J_i}\right)_{E=0} = \left(Z_i^* - \frac{V_i}{V_s}Z_s^*\right)|e| . \tag{25}$$

From this equation it is apparent that when a solute atom i is displaced in the binary mixture, the induced flux of charge is made of two parts: (i) Z_i^* due to the displacement of the solute atom itself; and (ii) $-(V_i/V_s)Z_s^*$ due to the backflow of electric charge associated with the motion of the solvent atom changing place with i in order to keep the volume constant. Equation (25) is general as it does not refer to any diffusion mechanism. Then in usual electrotransport experiments the apparent effective valence Z_i^{**} is measured rather than the true effective valence Z_i^*. The charge current Z_i^* induced by the motion of one solute atom can be written

$$Z_i^* = Z_i + Z_{ie}^* , \tag{26}$$

where Z_i is the bare ionic charge of species i, and $Z_{ie}^* = -(J_e/J_i)_{E=0,J_S=0}$ is the electric-charge flux due to the electrons driven by the moving impurity in a sample that is not subjected to an electric field. Conversely, it can be shown from the Onsager relations that $Z_i^*|e| = F^{(i)}/E$ is the drag force experienced by solute atoms when a unit electric field is applied to the sample. The force acting on an atom of species (i) can therefore be written

$$\vec{F}^{(i)} = Z_i|e|\vec{E} + \vec{F}_{ie} , \tag{27}$$

where $\vec{F}_{ie} = Z_{ie}^*|e|\vec{E}$ is the drag force exerted on i atoms by the electron gas.

From these considerations it is easy to calculate Z_i^{**} given by (25). As a first step we consider a sample of pure solvent whose resistivity is ρ_0. When a given current density is passed through the sample, the $N_s^0 Z_s$ electrons contained in a unit volume are subject to; (i) the electrostatic force $N_s^0(-Z_s|e|\rho_0\vec{j})$; and (ii) the force $-N_s^0\,\vec{F}_{se}$ opposite to the drag force exerted by the electron gas on the ions. The mechanical balance of these forces implies that

$$N_s^0(\vec{F}_{se} + Z_s|e|\rho_0\vec{j}) = 0 . \tag{28}$$

In a second step we consider a dilute binary alloy containing N_s and N_i solvent and solute atoms per unit volume, respectively. The resistivity of the mixture can be written

$$\rho = \rho_0 + \rho_i N_i , \tag{29}$$

where ρ_i is the specific resistivity of species (i) at low concentration in the solvent. When the same current density $\vec{j}$, as in the first step, is passed through the alloy, the mechanical balance of the forces acting on the electron gas

$$N_s\vec{F}_{se} + N_i\vec{F}_{ie} + (N_s Z_s + N_i Z_i)|e|\rho\vec{j} = 0 . \tag{30}$$

Using (24), this equation can be written

$$N_i\left[\left(\vec{F}_{ie} - \frac{V_i}{V_s}\vec{F}_{se}\right) + \left(Z_i - \frac{V_i}{V_s}Z_s\right)\rho|e|\vec{j}\right] = -\frac{1}{V_s}(\vec{F}_{se} + Z_s|e|\rho_0\vec{j} + Z_s|e|\rho_i N_i\vec{j}) . \tag{31}$$

Assuming that $\vec{F}_{se}$ and $\vec{F}_{ie}$ depend only on the current density $\vec{j}$, it is therefore straightforward to show that

$$Z_i^{**} = -N_s^0 Z\,(\rho_i/\rho) . \tag{32}$$

Hence, the apparent effective valence of solute atoms is entirely determined by their specific resistivity ρ_i in the host metal. Table V gives a test of expression (32) for a number of binary mixtures: for each alloy we give the pure solvent resistivity ρ_0, the specific resistivity $\rho_i' = \rho_i N_s^0$ of the solute in $\mu\Omega$ cm/at.%, the effective valence computed by Stroud,[7] Z^{**} calculated using (32) and the measured value of $Z.^{**}$ The experimental numbers are from the compilation of Pratt and Sellors[1]; a positive value for Z_i^{**} means that the apparent drift of the solute is directed towards the cathode. It is apparent from Table I that the

TABLE V. Apparent effective valence of solute atoms in a number of dilute binary alloys.

Solvent	Solute	T (°C)	ρ_0 ($\mu\Omega$ cm)	ρ_i' ($\mu\Omega$ cm/at. %)	Z_i^* (Ref. 7)	Z_i^{**} [Eq. (32)]	Z_i^{**} (exp.)
Na ($Z = 1$)	K	100	9.4	+0.9		-9.4	-10.6
	Cd	155	11.8	+4.5		-37.6	-43
	Hg	152	11.5	+6.4		-55.8	-50
	Sn	200	13.5	+11.7	-363	-86.0	-27
K ($Z = 1$)	Na	100	15.4	+1.2		-7.9	-0.5
Cu ($Z = 1$)	Sn	1153	24.0	+5.2		-21.8	-19.9
Ag ($Z = 1$)	Au	1100	18.5	+0.5		-2.5	<0
	Sn	992	17.6	+10.8		-61.2	-59.6
Cd ($Z = 2$)	Bi	350	34.0	+3.5		-20.6	-16.4
Hg ($Z = 1$)	Na	20	95.8	+0.6		-0.6	-0.4
	K	20	95.8	+4.1		-0.4	-1.2
	Ag	25	95.8	-3.9		+4.0	+1.5
	Au	25	95.8	-4.0		+4.1	+1.4
	Cd	27	96.0	-0.9		+0.9	+1.2
	In	20	95.8	-4.2		+4.3	>0
Ga ($Z = 3$)	Sn	20	25.6	+0.2		-2.5	-1.6
In ($Z = 3$)	Ag	700	45.0	+0.17		-1.1	-0.8
	Sn	166	33.4	+0.38	-1.16	-3.4	-2.8
	Bi	200	34.3	+1.14	-8.66	-10.0	-6.5
Sn ($Z = 4$)	Cu	350	50	+0.42		-3.4	-1.6
	Ag	630	57.9	+0.12		-0.8	-0.5
	Au	300	49.6	+0.32		-2.6	-2.2
	In	401	50	-0.15	+0.73	+1.2	+1.4
	Sb	401	50	+0.66		-5.3	-4.2
	Bi	300	49.6	+1.47	-8.25	-10.7	-2.0
Pb ($Z = 4$)	Ag	360	97	+0.23		-0.95	+0.5
	Au	450	101	+0.17		-0.16	-0.1
	Bi	500	103	+0.49	-2.1	-1.8	-0.8
Bi ($Z = 5$)	In	200	126	-0.65	+2.75	+2.5	>0
	Sn	500	143	-0.65	+2.40	+2.1	+1.1
	Pb	500	143	-0.23	+2.87	+0.8	>0

overall agreement between Stroud's calculations and the values of Z_i^{**} given by (32) is fairly good, and that both calculations give a good account of the experimental values. The sign of Z_i^{**} is especially well predicted by (32). As for its absolute value, all figures in Table V have been obtained assuming that the valence electrons of the solvent form a gas of free conduction electrons. This is a good assumption for alkali and noble host metals, but not for polyvalent metals where conduction may take place through electrons and holes.

V. CONCLUSION

In view of its remarkable simplicity it is gratifying that Eq. (32) accounts so well for the experimental results. With the exception of the system *Pb* Ag, the apparent effective valences calculated in Table V are in agreement with ex-

periment at least as regards sign. In a more elaborate theory one should calculate ρ_i' the residual resistivity of impurities, from first principles, using for instance a pseudopotential theory as did Stroud.[7] This kind of calculation is even more complicated than it is in solids because it requires the partial ionic structure factors in the liquid, for which measurements using neutron diffraction or estimation in some crude approximations are necessary.

Another interesting experimental result of the present work is the j^2 dependence of the effective diffusion coefficient and the absence of a threshold for the appearance of electroconvection. In the theory we give in Sec. III, we assume that the convection is initiated by an unbalance of electric drag forces in the neighborhood of the capillary surfaces. The thickness of the region affected by these unbalanced forces is rather small (~40 Å), but large enough to account for the drastic increase of the diffusion coefficient. Because this thickness is also too large on the atomic scale to be interpreted in terms of the properties of perfect surfaces, we think that the starting point of our calculation, namely, the expression (9) of the variation of the electron density should be considered as a simulation of complex phenomena taking place at the capillary surface. From an experimental point of view, the importance of such surface effects are currently investigated by varying the diameter of the capillary used in the shear cell described in Sec. II.

---

*Laboratoire associé au CNRS No. 155.

[1]J. N. Pratt and R. G. R. Sellors, *Electrotransport in Metals and Alloys* (Trans. Tech. Publications, Clausthal, Germany, 1973).
[2]H. B. Huntington and A. R. Grone, J. Phys. Chem. Solids 20, 76 (1961).
[3]C. Bosvieux and J. Friedel, J. Phys. Chem. Solids 23, 123 (1962).
[4]V. B. Fiks, Sov. Phys.-Solid State 1, 14 (1959).
[5]R. S. Sorbello, J. Phys. Chem. Solids 34, 937 (1973).
[6]L. Turban, P. Noziéres, and M. Gerl, J. Phys. (Paris) 37, 159 (1976).
[7]D. Stroud, Phys. Rev. B 13, 4221 (1976).
[8]W. F. Schaich, Phys. Rev. B 13, 3360 (1976).
[9]R. Landauer and J. W. F. Woo, Phys. Rev. B 10, 1266 (1974).
[10]A. Lodding, J. Phys. Chem. Solids 28, 557 (1967).
[11]D. K. Belaschenko, Russ. J. Phys. Chem. 39, 430 (1965).
[12]R. E. Shaw and J. D. Verhoeven, Metall. Trans. 4 2349 (1973).
[13]L. Schmidt and J. D. Verhoeven, Trans. Am. Inst. Min. Eng. 239, 148 (1967).
[14]A. Lodding and A. Klemm, Z. Naturforschung 17a, 1085 (1962).
[15]S. A. Regirer, Zh. Prikl. Mekh. Tekh. Fiz. 15, 15 (1962).
[16]G. E. Pikus and V. B. Fiks, Sov. Phys.-Solid State 1, 972 (1959).
[17]N. H. Nachtrieb, Adv. Phys. 16, 309 (1967).
[18]D. A. Rigney, *Liquid Metals*, Int. Phys. Conf. Ser. No 30 (The Institute of Physics, Bristol, 1976), p. 619.
[19]D. Agnoux, thesis (Université Nancy, 1976) (unpublished).
[20]J. M. Escanye, thesis (Université Nancy, 1977) (unpublished).
[21]J. W. Westhaver, J. Res. Natl. Bur. Stand. 38, 169 (1947).
[22]V. B. Fiks, Sov. Phys.-Tech. Phys. 27, 1176 (1957).
[23]J. M. Escanye, M. Gerl, Phys. Lett. A 63, 35 (1977).